IEEE Robotics and Automation Letters (RA-L) paper, presented at ICRA 2026, Vienna, Austria. Cite as RA-L paper.

Energy-shaping Controller for Time-invariant Multiple Contacts

Ehtisham ul Hasan[1] and Angelika Peer[2]

Abstract— **While in the past industrial robots were strictly separated from humans, today robots serve humans in a variety of industrial applications that also involve close or even physical human-robot interaction. Hereby, safety is of utmost importance and thus, the design of the control system needs to ensure a stable and safe operation. In this context, safety has been mainly addressed for single interaction points. In this article, we present an energy shaping controller that is capable of ensuring safety even in the case of multiple human contact points that may occur when co-manipulating an object. The presented approach is tested and validated in experiments. Results indicate that for the studied co-manipulation task involving time-invariant multiple human contacts, a safe interaction can be achieved.**

I. INTRODUCTION

Today, robots collaborate with humans in a range of industrial applications and some of them may also require robots to operate in close interaction with humans or to interact with them directly or via objects. Hereby, contacts may occur intentionally or unintentionally. In all cases, safety is of utmost importance to prevent harmful events.

Safety standards for human-robot collaborative operation can be found in the technical specification ISO/TS 15066 [1]. It defines four different operation modes 1) safety-rated monitored stop, 2) hand-guiding, 3) speed and separation monitoring as well as 4) power and force limiting to guarantee safe human-robot interaction. The latter mode allows for contact between human and robot if power and force at the contact points can be guaranteed to remain below certain thresholds, e.g. by exploiting special control techniques.

The Port-Hamiltonian (PH) framework has been found useful for modeling systems and their interactions and it has been also widely used to develop different types of safety-related energy shaping controllers [2], [3], [4], [5], [6]. The framework allows to represent a system in terms of energy variables and to break it down into independent sub-systems with the help of the port concept. The individual sub-systems can then be coupled with each other via power ports to build more complex systems, whereby the subsystems can exchange energy with each other.

*This study is supported by the Interconnected Nord-Est Innovation Ecosystem (iNEST) and received funding from the European Union Next-GenerationEU (PIANO NAZIONALE DI RIPRESA E RESILIENZA (PNRR) – MISSIONE 4 COMPONENTE 2, INVESTIMENTO 1.5 – D.D. 1058 23/06/2022, ECS00000043). This manuscript reflects only the authors' views and opinions, neither the European Union nor the European Commission can be considered responsible for them.

[1]Ehtisham ul Hasan is with Faculty of Engineering, Free University of Bozen-Bolzano, 39100, Italy ehtishamul.hasan@unibz.it

[2]Angelika Peer is with Faculty of Engineering, Free University of Bozen-Bolzano, 39100, Italy angelika.peer@unibz.it

In [3], authors for example presented an energy-based safety controller that shapes the energy and power over a single contact point with the human and keeps power and energy below certain thresholds to prevent harmful behaviours of the robot. In addition to shaping the energy at the human interaction port, a model for estimating muscle fatigue has been considered. Similarly, but more recently, the authors in [7] proposed an energy-shaping controller that limits the kinetic energy exchanged during collisions and the potential energy during clamping scenarios. However, for both works, the authors focused only on a single interaction point.

In [2], authors considered a human-robot team interaction in which the human commands the overall behaviour of a robot consisting of two KUKA LWR cooperative manipulator arms mounted on a mobile base via hand gestures, while the robot manipulators are controlled to comply with formation constraints to be able to hold and transport an object. Authors modelled the overall system as Port-Hamiltonian system and exploited the related energy function to enhance safety. The developed controller was tested in simulation and in experiments for maintaining the desired constrained system formation while achieving the desired energy-shaping behaviour. The proposed approach again considers only one interaction point with the human, whereby in this particular case even only a virtual and no real physical interaction point was considered.

Energy and power exchange over single interaction points have been studied also in [8] and [9], where a human interacted with a single and multi-DOF robot, respectively. The authors presented a safety and energy-aware impedance controller for collaborative robots. The controller allows to enforce energy and power limitations to ensure safe human-robot interaction for single human contact points.

The Port-Hamiltonian (PH) formulation facilitates an energy-based analysis by expressing system dynamics in terms of energy variables and power ports, providing a well-suited energy-based representation of physical human-robot interaction. Unlike conventional modeling techniques, PH systems natively encode energy storage, dissipation, and transfer, enabling structured, modular interconnections and controller designs that respect physical energy limits. This is particularly beneficial in safety-critical applications, where compliance and energy and power limits must be guaranteed. Without the PH formulation, ensuring such behavior in multi-contact scenarios would be significantly more complex.

Summarizing, energy and power limiting concepts are well known in literature, but are so far mainly applied to situations with a single interaction point. In this article, we

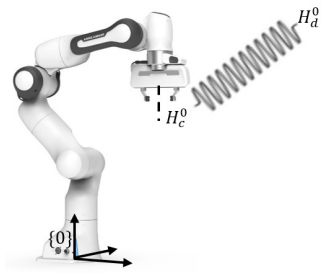

Fig. 1. Frame of reference for single human contact point and a virtual spring connected between the current and desired end-effector configurations.

aim at extending the concept of [9] to multiple human contact points, by exploiting the Port-Hamiltonian framework and combining it with the concept of the grasp matrix for developing an energy-shaping controller. The final control scheme shapes the energy flow at multiple time-invariant human contact points during the execution of a co-manipulation task.

This article is organized as follows. Section II introduces the new control scheme, while Section III evaluates it in real experiments. Conclusions are drawn in section IV.

II. Energy Shaping Controller

In the following subsections, we first briefly review the energy shaping controller for a single interaction point as presented in literature, while then we report its needed extensions to account for the case of multiple human interaction points occurring when commonly handling an object.

A. Energy Shaping Controller for Single Interaction Point

1) Impedance Control: Following [9], an impedance control scheme is formulated within the Port-Hamiltonian framework allowing to describe the system in terms of stored energy and power passing over interaction points and to control both of them with the help of an energy-shaping controller.

The current and desired homogeneous configurations of the robot end-effector are considered hereby to be connected via a multidimensional virtual spring, see Fig. 1, whereby the current and desired configurations of the robot end-effector are given by $\{c\}$ and $\{d\}$.

The current and desired configuration of the robot end-effector can be described with respect to the base frame $\{0\}$ of the robot with the help of homogeneous transformations, $\mathbf{H}_c^0 \in \mathbb{R}^{4\times4}$ and $\boldsymbol{H}_d^0 \in \mathbb{R}^{4\times4}$, respectively. Similarly, the human contact can be described by the homogeneous transformation $\mathbf{H}_{hc}^0 \in \mathbb{R}^{4\times4}$. The wrench exerted by the virtual spring of the impedance controller, is considered a function of the relative configuration $\boldsymbol{H}_d^c \in \mathbb{R}^{4\times4}$, between the current and desired pose of the robot end-effector (see Fig. 1) and can be defined as

$$\boldsymbol{H}_d^c = (\boldsymbol{H}_c^0)^{-1} \cdot \boldsymbol{H}_d^0 = \begin{pmatrix} \boldsymbol{R}_d^c & \boldsymbol{p}_d^c \\ \mathbf{0}^T & 1 \end{pmatrix}. \tag{1}$$

With the help of this relative configuration the wrench acting on the robot end-effector due to the virtual spring of the impedance controller is given by [10]:

$$\tilde{\boldsymbol{m}} = -2as(\boldsymbol{G}_o\boldsymbol{R}_d^c) - as(\boldsymbol{G}_t\boldsymbol{R}_c^d\tilde{\boldsymbol{p}}_d^c\tilde{\boldsymbol{p}}_d^c\boldsymbol{R}_d^c) - 2as(\boldsymbol{G}_c\tilde{\boldsymbol{p}}_d^c\boldsymbol{R}_d^c), \tag{2}$$

$$\tilde{\boldsymbol{f}} = -\boldsymbol{R}_c^d as(\boldsymbol{G}_t\tilde{\boldsymbol{p}}_d^c)\boldsymbol{R}_d^c - as(\boldsymbol{G}_t\boldsymbol{R}_c^d\tilde{\boldsymbol{p}}_d^c\boldsymbol{R}_d^c) - 2as(\boldsymbol{G}_c\boldsymbol{R}_d^c), \tag{3}$$

where, $\tilde{\boldsymbol{m}}$ refers to the torques and $\tilde{\boldsymbol{f}}$ to the forces, both expressed in robot end-effector frame $\{c\}$, hence the wrench vector can be written as $\boldsymbol{W}_c^c = [\boldsymbol{f} \quad \boldsymbol{m}]^T$. Hereby, $\tilde{\boldsymbol{p}}$ refers to the corresponding vector's skew-symmetric matrix, and the as() operator refers to the skew-symmetric part of a square matrix. The matrices $\boldsymbol{G}_t$, $\boldsymbol{G}_o$ and $\boldsymbol{G}_c$ all $\in \mathbb{R}^{3\times3}$, define the co-stiffness matrices and are responsible for defining the initial potential energy of the system and are computed with the help of the symmetric translational $\boldsymbol{K}_t \in \mathbb{R}^{3\times3}$, rotational $\boldsymbol{K}_o \in \mathbb{R}^{3\times3}$ and $\boldsymbol{K}_c \in \mathbb{R}^{3\times3}$ coupling stiffnesses as follows:

$$\boldsymbol{G}_x = \frac{1}{2}tr(\boldsymbol{K}_x)\boldsymbol{I}_3 - (\boldsymbol{K}_x) \quad \text{with} \quad x \in \{t, o, c\}, \tag{4}$$

where $\boldsymbol{I}_n \in \mathbb{R}^{n\times n}$ refers to the identity matrix. By applying a coordinate transformation, the wrench given in the end-effector frame can be expressed in the robot base frame $\{0\}$ by

$$\boldsymbol{W}_c^0 = -Ad_{\boldsymbol{H}_c^0}^T\boldsymbol{W}_c^c, \tag{5}$$

where $\boldsymbol{W}_c^0 \in \mathbb{R}^{6\times1}$ denotes the wrench exerted by the impedance controller due to the virtual spring attached between the current and desired configuration of the robot end-effector and expressed in the robot base frame $\{0\}$ and Ad() represents the Adjoint of a matrix.

Thus, the corresponding robot command torque $\boldsymbol{\tau}_c \in \mathbb{R}^{7\times1}$ can be determined with the Jacobian transpose as follows:

$$\boldsymbol{\tau}_c = \boldsymbol{J}^T(\boldsymbol{q})\boldsymbol{W}_c^0 - \boldsymbol{B}\dot{\boldsymbol{q}}, \tag{6}$$

where $\boldsymbol{J} \in \mathbb{R}^{6\times7}$ is the robot Jacobian, $\boldsymbol{B} \in \mathbb{R}^{7\times7}$ refers to the damping added to each joint of the robot manipulator in joint space to adjust the robot dynamic behaviour and $\dot{\boldsymbol{q}} \in \mathbb{R}^{7\times1}$ is the joint velocity.

2) Safety-aware Variable Impedance Control: To guarantee safety, first the energy stored in the system needs to be considered, as in adverse situations it may be dissipated over the human contact point. The Hamiltonian energy function E is given by the kinetic energy of the robot and the potential energy stored in the robot.

Thus, the total energy can be expressed as follows:

$$E_{tot} = \quad T_k(\boldsymbol{q}, \dot{\boldsymbol{q}}) + V_p(\boldsymbol{R}_d^c, \boldsymbol{p}_d^c), \tag{7}$$

whereby the kinetic energy of the robot $T_k(\boldsymbol{q}, \dot{\boldsymbol{q}})$ is given by:

$$T_k(\boldsymbol{q}, \dot{\boldsymbol{q}}) = \frac{1}{2}\dot{\boldsymbol{q}}^T\boldsymbol{M}(\boldsymbol{q})\dot{\boldsymbol{q}}. \tag{8}$$

Similarly, the potential energy stored in the virtual spring of the impedance controller can be calculated as follows:

$$V_p(\boldsymbol{R}_d^c, \boldsymbol{p}_d^c) = V_t(\boldsymbol{R}_d^c, \boldsymbol{p}_d^c) + V_o(\boldsymbol{R}_d^c) + V_c(\boldsymbol{R}_d^c, \boldsymbol{p}_d^c), \quad (9)$$

where $V_t(\boldsymbol{R}_d^c, \boldsymbol{p}_d^c)$, $V_o(\boldsymbol{R}_d^c)$ and $V_c(\boldsymbol{R}_d^c, \boldsymbol{p}_d^c)$ are the translational, orientational and coupling element of the potential energy and are computed following [10]:

$$\begin{aligned} V_t(\boldsymbol{R}_d^c, \boldsymbol{p}_d^c) &= -\frac{1}{4} tr(\tilde{\boldsymbol{p}}_d^c \boldsymbol{G}_t \tilde{\boldsymbol{p}}_d^c) - \frac{1}{4} tr(\tilde{\boldsymbol{p}}_d^c \boldsymbol{R}_d^c \boldsymbol{G}_t \boldsymbol{R}_c^d \tilde{\boldsymbol{p}}_d^c), \\ V_o(\boldsymbol{R}_d^c) &= -tr(\boldsymbol{G}_o \boldsymbol{R}_d^c), \\ V_c(\boldsymbol{R}_d^c, \boldsymbol{p}_d^c) &= tr(\boldsymbol{G}_c \boldsymbol{R}_c^d \tilde{\boldsymbol{p}}_d^c). \end{aligned} \quad (10)$$

Then, following [11], [12] the amount of potential energy $V_p(\boldsymbol{R}_d^c, \boldsymbol{p}_d^c)$ that the virtual spring can supply to the system can be regulated to remain below desired thresholds to assure safety. This is possible since the components of the potential energy in (10) are proportional to the co-stiffness matrices $\boldsymbol{G}_t$, $\boldsymbol{G}_o$ and $\boldsymbol{G}_c$ [9]. Choosing an initial set of co-stiffness matrices and scaling these co-stiffness matrices with a scaling parameter λ such that $\boldsymbol{G}_x = \lambda \boldsymbol{G}_{x_u}$ (for $x = t, o, c$) with:

$$\lambda = \begin{cases} 1 & \text{if } E_{tot} \leq E_{max}, \\ \frac{E_{max} - T_k(\boldsymbol{q}, \dot{\boldsymbol{q}})}{V_{p_u}(\boldsymbol{R}_d^c, \boldsymbol{p}_d^c)} & \text{otherwise}, \end{cases} \quad (11)$$

allows the total energy in the system to be limited to a maximum energy E_{max}. Hereby the index $\{\mathrm{u}\}$ refers to the unscaled co-stiffness matrices and related potential energy. Once the scaling parameter λ is adjusted, the energy stored in the system is given by:

$$E_{tot} = T_k(\boldsymbol{q}, \dot{\boldsymbol{q}}) + \lambda V_{p_u}(\boldsymbol{R}_d^c, \boldsymbol{p}_d^c). \quad (12)$$

Next, to limit the rate of the transfer of energy (power) to the human collaborator, the power that can be transferred to the human needs to be limited. In this regard, given the applied wrench at the human contact $\boldsymbol{W}_{hc}^{hc} \in \mathbb{R}^{6\times 1}$, and the wrench applied by the impedance controller $\boldsymbol{W}_c^c$, the power supposed to be dissipated via the human contact point defined as P_{hc} can be computed by:

$$P_{hc} = -(\boldsymbol{J}^T(\boldsymbol{q}) \boldsymbol{W}_c^0 - \boldsymbol{B}\dot{\boldsymbol{q}})^T \dot{\boldsymbol{q}}. \quad (13)$$

The power dissipation via the contact point is regulated by adjusting the damping parameter β [11], [12]. The power dissipation at the human contact point can be limited to a maximum P_{max} by choosing β as follows:

$$\beta = \begin{cases} \frac{P_{max} + (\boldsymbol{J}^T(\boldsymbol{q}) \boldsymbol{W}_c^0)^T \dot{\boldsymbol{q}}}{\dot{\boldsymbol{q}}^T \boldsymbol{B}_u \dot{\boldsymbol{q}}} & \text{if } P_{hc} < P_{max}, \\ 1 & \text{otherwise}, \end{cases} \quad (14)$$

with

$$\boldsymbol{B} = \beta \boldsymbol{B}_u. \quad (15)$$

where $\boldsymbol{B}$ is the new joint damping matrix calculated with the help of the scaling parameter β and the unscaled joint damping matrix $\boldsymbol{B_u}$.

3) Passivity through Energy Tanks: Finally, passivity and with this stability of the control scheme is guaranteed by the introduction of energy tanks [9]. They are needed since the safety-related scaling of the impedance parameters can result in loss of passivity of the system. In total, n energy tanks are defined, corresponding to the number of degrees of freedom of the controllable joints. Each energy tank is modeled as a spring $H(s)_n = \frac{1}{2} k s^2$ with constant stiffness ($k = 1$) connected to the robot through a transmission. This transmission is responsible for allowing the power to flow from the controller to the robot and is regulated by the ratio u that is computed using

$$u_n = \begin{cases} \frac{-\tau_{c_n}}{s_n} & \text{if } H_n(s_n) > \epsilon, \\ \frac{-\tau_{c_n}}{\gamma^2} s_n & \text{otherwise}, \end{cases} \quad (16)$$

where $\gamma = \sqrt{2\epsilon}$ and ϵ is the minimum amount of energy in the tank before the robot and the controller are decoupled and τ_{c_n} is the torque computed by the control scheme for each degree of freedom. Once the transmission ratio is adjusted in accordance to the energy levels in the energy tanks $H_n(s)$, the final control torque to be sent to joint n is given by

$$\tau_n = -u_n \cdot s_n. \quad (17)$$

As a result power can only flow from the controller to the robot if there is still energy left in the tank, which guarantees passivity.

B. Energy Shaping Controller for Multiple Interaction Points

As main contribution of this work we present an energy-shaping controller that besides controlling the total energy in the system, allows to control the energy flows (power) over not only one, but *multiple* human interaction points. The controller ensures safety by limiting power and energy such that they remain below admissible limits as defined in the safety standard ISO/TS 15066 for collaborative robots.

We consider all physical contacts to be rigid and time-invariant. Without restriction of generality, we consider the human to touch the object at two contact points, referred to as left human contact (lhc) and right human contact (rhc) and the robot to grasp the object at a single interaction point (c), see Fig. 2. In the following paragraphs, we highlight the changes to be applied to the aforementioned algorithm for a single interaction point, when aiming for shaping energy over multiple interaction points.

Thus, instead of a single human contact wrench, we now have multiple ones: a wrench $\boldsymbol{W}_{lhc}^{lhc}$ acting on the left human contact point and $\boldsymbol{W}_{rhc}^{rhc}$ acting on the right human contact point, both expressed in the robot base frame by:

$$\boldsymbol{W}_{lhc}^0 = -Ad_{\boldsymbol{H}_{lhc}^0}^T \boldsymbol{W}_{lhc}^{lhc}, \quad (18)$$

$$\boldsymbol{W}_{rhc}^0 = -Ad_{\boldsymbol{H}_{rhc}^0}^T \boldsymbol{W}_{rhc}^{rhc}. \quad (19)$$

In addition, the total energy of the system, cf. (7), needs to account for the kinetic and potential energy stored in the

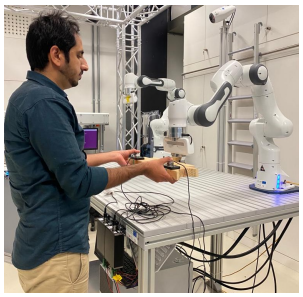

(a)

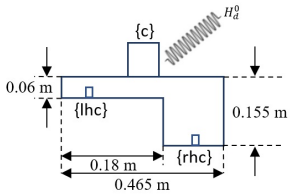

(b)

Fig. 2. (a) Co-manipulation task with multiple human contacts, (b) Frame of reference for multiple human contact points and the robot contact point and a virtual spring connected between the current and desired end-effector configurations.

jointly manipulated object. Thus, the total energy can be expressed as follows:

$$E_{tot} = T_k(\boldsymbol{q},\dot{\boldsymbol{q}}) + T_{k,obj}(\dot{\boldsymbol{p}}^0_{obj},\boldsymbol{\omega}^0_{obj}) + V_p(\boldsymbol{R}^c_d,\boldsymbol{p}^c_d) + V_{p,obj}(\boldsymbol{p}^0_{obj}), \quad (20)$$

whereby the kinetic energy of the object $T_{k,obj}(\dot{\boldsymbol{p}}^0_{obj},\boldsymbol{\omega}^0_{obj})$ is given by:

$$T_{k,obj}(\dot{\boldsymbol{p}}^0_{obj},\boldsymbol{\omega}^0_{obj}) = \frac{1}{2}m_{obj}(\dot{\boldsymbol{p}}^0_{obj})^T\dot{\boldsymbol{p}}^0_{obj} + \frac{1}{2}(\boldsymbol{\omega}^0_{obj})^T\boldsymbol{I}_{obj}\boldsymbol{\omega}^0_{obj}, \quad (21)$$

with m_{obj} the mass of the object, $\boldsymbol{I}_{obj}$ the inertia tensor, $\dot{\boldsymbol{p}}^0_{obj}$ the translational and $\boldsymbol{\omega}^0_{obj}$ the rotational velocity of the center of mass of the handled object. The potential energy of the object is determined by:

$$V_{p,obj}(\boldsymbol{p}^0_{obj}) = m_{obj}\boldsymbol{g}^T\boldsymbol{p}^0_{obj}, \quad (22)$$

with $\boldsymbol{p}^0_{obj}$ the position of the center of mass of the handled object with respect to the base of the robot.

Consequently, the scaling parameter λ in (11) needs to be replaced with:

$$\lambda = \begin{cases} 1 & \text{if } E_{tot} \le E_{max}, \\ \frac{E_{max} - T_k(\boldsymbol{q},\dot{\boldsymbol{q}}) - T_{k,obj}(\boldsymbol{p}^0_{obj},\boldsymbol{\omega}^0_{obj}) - V_{p,obj}(\boldsymbol{p}^0_{obj})}{V_{p_u}(\boldsymbol{R}^c_d,\boldsymbol{p}^c_d)} & \text{otherwise}, \end{cases} \quad (23)$$

and the adjusted energy in the system (12) with:

$$E_{tot} = T_k(\boldsymbol{q},\dot{\boldsymbol{q}}) + T_{k,obj}(\dot{\boldsymbol{p}}^0_{obj},\boldsymbol{\omega}^0_{obj}) + V_{p,obj}(\boldsymbol{p}^0_{obj}) + \lambda V_{p_u}(\boldsymbol{R}^c_d,\boldsymbol{p}^c_d). \quad (24)$$

Since we finally have more than one human contact point, the transfer rate of energy (power), cf. (13) needs to be limited via all of the multiple time-invariant human contact points. The power equation can be formulated as follows:

$$P_{obj} = P_c + P_{lhc} + P_{rhc}, \quad (25)$$

with $P_c = \boldsymbol{\tau}_c^T\dot{\boldsymbol{q}}$ referring to the power injected into the system by the robot controller. Rearranging (25), the power transfer at the left and right human contacts can be computed by:

$$P_{lhc} = \boldsymbol{W}^0_{obj}\dot{\boldsymbol{X}} - (\boldsymbol{J}^T(\boldsymbol{q})\boldsymbol{W}^0_c - \boldsymbol{B}\dot{\boldsymbol{q}})^T\dot{\boldsymbol{q}} - \boldsymbol{W}^0_{rhc}\dot{\boldsymbol{X}}, \quad (26)$$

$$P_{rhc} = \boldsymbol{W}^0_{obj}\dot{\boldsymbol{X}} - (\boldsymbol{J}^T(\boldsymbol{q})\boldsymbol{W}^0_c - \boldsymbol{B}\dot{\boldsymbol{q}})^T\dot{\boldsymbol{q}} - \boldsymbol{W}^0_{lhc}\dot{\boldsymbol{X}}, \quad (27)$$

where $\dot{\boldsymbol{X}} = [\dot{\boldsymbol{p}}^0_{obj} \quad \boldsymbol{\omega}^0_{obj}]^T$ and $\boldsymbol{W}^0_{lhc}$ stand for the applied wrench at the left human contact, $\boldsymbol{W}^0_{rhc}$ for the applied wrench at the right human contact, $\boldsymbol{W}^0_c$ for the wrench applied by the impedance controller, and $\boldsymbol{W}^0_{obj}$ for the resultant wrench at the center of mass of the held object. Similar to (14), the power at the left P_{lhc} and right P_{rhc} human contact points can finally be limited to a maximum P_{max} by choosing β as follows:

$$\beta = \begin{cases} \frac{P_{max} - \boldsymbol{W}^0_{obj}\dot{\boldsymbol{X}} + (\boldsymbol{J}^T(\boldsymbol{q})\boldsymbol{W}^0_c)^T\dot{\boldsymbol{q}} + \boldsymbol{W}^0_{rhc}\dot{\boldsymbol{X}}}{\dot{\boldsymbol{q}}^T\boldsymbol{B}_u\dot{\boldsymbol{q}}} & \text{if } P_{lhc} < P_{max}, \\ \frac{P_{max} - \boldsymbol{W}^0_{obj}\dot{\boldsymbol{X}} + (\boldsymbol{J}^T(\boldsymbol{q})\boldsymbol{W}^0_c)^T\dot{\boldsymbol{q}} + \boldsymbol{W}^0_{lhc}\dot{\boldsymbol{X}}}{\dot{\boldsymbol{q}}^T\boldsymbol{B}_u\dot{\boldsymbol{q}}} & \text{if } P_{rhc} < P_{max}, \\ 1 & \text{otherwise.} \end{cases} \quad (28)$$

Please note that this way we limit the dissipated power at the multiple human contact points and not the injected power by the robot.

Finally, the resultant wrench $\boldsymbol{W}^0_{obj} \in \mathbb{R}^{6\times1}$ required in (26)-(28) and applied at the center of mass of the held object can be obtained with the help of the grasp matrix and the wrenches applied at the different grasping points. In this regard, we assume that (i) the robot and the human are interacting indirectly via a rigid object of known geometry (ii) the human is grasping the object at multiple known time-invariant contact points, and (iii) given the center of mass of the held object, the position vectors from the center of mass of the object to the left human contact point $\boldsymbol{p}^{obj}_{lhc}$ and the right human contact point $\boldsymbol{p}^{obj}_{rhc}$ can be determined. Similarly, the position vector from the center of mass of the held object to the robot contact point $\boldsymbol{p}^{obj}_c$, can be computed. Next, the skew symmetric matrices $\tilde{\boldsymbol{p}}^{obj}_{lhc}$, $\tilde{\boldsymbol{p}}^{obj}_{rhc}$ and $\tilde{\boldsymbol{p}}^{obj}_c$ are derived from the respective position vectors [13], [14] and the following grasp matrices are formulated:

$$\boldsymbol{\mathcal{G}}_{\boldsymbol{obj,lhc}} = \begin{bmatrix} \boldsymbol{I}_3 & \boldsymbol{0}_3 \\ \tilde{\boldsymbol{p}}^{obj}_{lhc} & \boldsymbol{I}_3 \end{bmatrix}, \quad \boldsymbol{\mathcal{G}}_{\boldsymbol{obj,rhc}} = \begin{bmatrix} \boldsymbol{I}_3 & \boldsymbol{0}_3 \\ \tilde{\boldsymbol{p}}^{obj}_{rhc} & \boldsymbol{I}_3 \end{bmatrix}, \quad (29)$$

$$\boldsymbol{\mathcal{G}}_{\boldsymbol{obj,c}} = \begin{bmatrix} \boldsymbol{I}_3 & \boldsymbol{0}_3 \\ \tilde{\boldsymbol{p}}^{obj}_c & \boldsymbol{I}_3 \end{bmatrix}, \quad (30)$$

where $\boldsymbol{\mathcal{G}}_{\boldsymbol{obj,lhc}}$ and $\boldsymbol{\mathcal{G}}_{\boldsymbol{obj,rhc}}$ both $\in \mathbb{R}^{6\times6}$ represent the grasp matrices for the left and right human contacts, both expressed with respect to the center of mass of the held object. Finally, the grasp matrix that defines the relative position of the robot contact with respect to the center of mass of the held object is given by $\boldsymbol{\mathcal{G}}_{\boldsymbol{obj,c}} \in \mathbb{R}^{6\times6}$. Thus, the resultant wrench $\boldsymbol{W}^0_{obj}$ applied at the center of mass of the handled object is given by:

$$\boldsymbol{W}^0_{obj} = -Ad^T_{\boldsymbol{H}^0_{obj}}(\boldsymbol{\mathcal{G}}_{\boldsymbol{obj,c}}\boldsymbol{W}^c_c + \boldsymbol{\mathcal{G}}_{\boldsymbol{obj,lhc}}\boldsymbol{W}^{lhc}_{lhc} + \boldsymbol{\mathcal{G}}_{\boldsymbol{obj,rhc}}\boldsymbol{W}^{rhc}_{rhc}). \quad (31)$$

It is important to note that the impact of singular configurations on the robot's movement are well handled in our proposed formulation. The energy-shaping controller computes control torques using the Jacobian transpose (6) rather than its inverse. This design choice avoids the numerical instabilities typically associated with matrix inversion near singular configurations, where the Jacobian becomes ill-conditioned.

Notably, at kinematic singularities, joint torques mapped through the Jacobian transpose result in zero, inherently limiting actuation. To be able to dissipate eventual excessive energy in the system, in the vicinity of singularities, joint-space damping remains active, continuously dissipating energy, while the energy tank mechanism limits the total energy that can be injected into the system. Stability and safety are thus ensured through a combination of joint-space damping, energy modulation via the energy-scaling mechanism (23), and strict passivity enforcement using energy tanks (16, 17).

III. Experimental Evaluation

A. Experimental setup

The energy-shaping controller for multiple time-invariant human contacts has been validated in experiments performed with a 7-DOF Franka Emika robot. An object of mass 0.4 kg was co-manipulated by a human and a Franka Emika robot. The human grasped the object at one side via multiple contact points, whereby the robot grasped it with its end-effector at the other side (see Fig. 2(b)). The robot was commanded to follow a pre-defined Cartesian trajectory, while considering two experimental conditions, namely manipulation of the object with (i) human acting as passive follower, and (ii) human acting as an active collaborator.

The different phases of the experiment are reported in Table I for a better understanding of the performed co-manipulation task.

The proposed controller was initially developed in Matlab Simulink, but was then moved to libfranka C++ due to encountered limitations of the Franka Matlab interface in integrating third-party sensor signals.

The human wrenches applied at each of the multiple human contact points were determined with the help of force/torque sensors. For this purpose, two six-axis force/torque sensors from ATI Automation (Nano25 and Mini27 Titanium) were attached to the object to be co-manipulated and data was acquired using a National Instruments Data Acquisition Card NI PCIe-6363 and Simulink Desktop Real-Time on a Windows PC. The sensor data acquired was then passed via the User Datagram Protocol (UDP) from the Windows machine to the Linux Workstation running the energy-shaping controller in libfranka C++. A diagram of the setup is depicted in Fig. 3.

The maximum allowable energy to be stored in the system was set to $E_{max} = 0.6$ J, whereby the maximum injected power at robot side to $P_{max} = 1.5$ W and the maximum

TABLE I

Phases of the co-manipulation task

0 <t <5 s	5 <t <10 s	t >10 s
Passive follower		
Robot prepares for grasping	Object grasped	Human acting as passive follower
Active human collaborator		
Robot prepares for grasping	Object grasped	Human acting as active collaborator

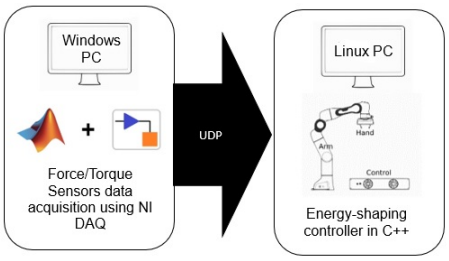

Fig. 3. System overview

allowable power to be dissipated via the multiple human contact points to $P_{max} =$ -1.5 W. They depend on the application and the critical body parts that may be affected and can be chosen according to ISO/TS 15066 (for illustration purposes rather low values have been chosen here). The gains of the controller were chosen to be $\boldsymbol{K}_t = 2000 \cdot \boldsymbol{I}_3$ N/m, $\boldsymbol{K}_0 = 320 \cdot \boldsymbol{I}_3$ Nm/rad, $\boldsymbol{K}_c = \boldsymbol{0}_3$ N/rad and $\boldsymbol{B}_u = 10 \cdot \boldsymbol{I}_7$ Ns/m. The maximum stiffness parameters were chosen such that a good tracking performance could be obtained when no thresholds were hit, while the damping was chosen to allow for the activation of significant damping to dissipate energy with the help of the controller in case needed. These latter parameters were tuned manually.

B. Experimental results

The proposed energy-shaping controller was found to successfully limit the energy stored in the system and the power that can be exchanged with the human via the multiple human contacts. Various Cartesian trajectories were tested to validate the proposed energy shaping controller. Here we present and discuss the results obtained for the following Cartesian trajectory:

$$\boldsymbol{H}_d^0 = \begin{cases} \boldsymbol{p}_d^0 = \begin{bmatrix} x \\ y(t) \\ z(t) \end{bmatrix} = \begin{bmatrix} 0.5071 \\ 0.3\sin(\theta t) \\ 0.29 \end{bmatrix} \\ \boldsymbol{R}_d^0 = \begin{bmatrix} 0.707 & -0.707 & 0.0 \\ -0.707 & -0.707 & 0.0 \\ 0.0 & 0.0 & -1.0 \end{bmatrix} \end{cases} \tag{32}$$

with $\theta = \frac{\pi}{4}(1 - \cos(\frac{\pi}{5})t)$.

C. Perfect passive follower

In case of the perfect passive follower, the human tries to perfectly follow the robot movements by exerting as little forces as possible during the co-manipulation task.

The power transferred over the left and right human contacts as well as the levels of the energy tanks were analyzed over the complete execution of the co-manipulation task. The total energy stored in the system, the power passing over each of the multiple human contacts as well as the control parameters λ and β were studied. The energy and power, as observed in experiments did not reach the thresholds and consequently the scaling parameters λ and β were found to remain at one throughout the whole execution of the co-manipulation task, see the accompanying video for details.

D. Active human collaborator

Next, we analyzed the controller behavior for the case of an active human collaborator who co-manipulates a grasped object together with the robot via multiple, time-invariant contact points. Three cases were considered for a better illustration of the controller capabilities: (I) a wrench is applied only via the left human contact, (II) a wrench is applied only via the right human contact, (III) a wrench is applied via two time-invariant human contacts. For each of the three cases, the active human collaboration phase started at 10 seconds.

For case (I) and case (II), the controller exhibited dynamic adaptation of the control parameters λ and β to regulate energy and power, respectively, in accordance with predefined safety thresholds. The observed behavior aligns with findings reported in state-of-the-art studies involving single interaction points [15], [16]. As these results do not constitute the primary focus of this work, detailed outcomes are omitted, but the cases are included in the accompanying video.

The experimental results related to case (III), in which wrenches were applied via multiple time-invariant human contacts are depicted in Fig. 4. As can be seen the robot end-effector position deviates from the desired path as long as the human wrench is actively applied. At around 12 s the thresholds for power allowed to dissipate (power to be dissipated by human defined as negative) are reached at the left and right human contact points and thus, the control parameter β is adjusted. This increases the tracking error, which again increases the energy stored in the virtual stiffness of the impedance controller as reflected in increasing levels of the energy tanks related to joints responsible for tracking the reference motion. Similar behavior has also been observed in state-of-the-art literature with a single interaction point [15], [16]. This increase in the energy levels increases also the total energy stored in the system. Thus, the energy threshold gets activated shortly after, which again results in the adaptation of the control parameter λ. Once the external human wrenches are removed (human starts again to follow the robot movements), the tracking error reduces and with this the energy stored in the system. At the end of the task, both human and robot contribute to decelerating the object to bring it to rest. Doing so, the power dissipated through left and right human contacts reach again the maximum admissible power limit to be dissipated (observed at around 24 s). Again the power is limited by adjusting the control parameter β, after which the object comes to rest and the control parameters return to their default values.

To better compare our results with the state-of-the-art literature, further experiments for case (III) were conducted:

1) Limiting injected versus dissipated power: In this section, we compare the state-of-the-art approach that limits the injected power at the robot side (Fig. 5) with our proposed approach that limits the dissipated power at the multiple time-invariant human contact points (Fig. 4). For this purpose, the human co-manipulated a jointly held asymmetrical

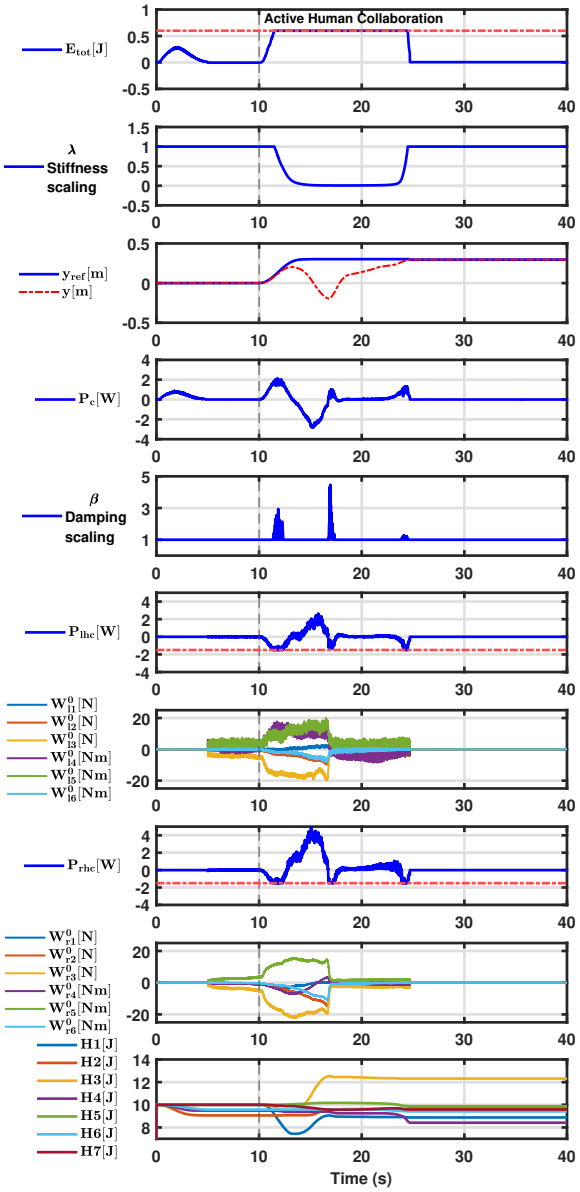

Fig. 4. Experimental results for limiting power dissipation via multiple (left and right) time-invariant human contacts during the co-manipulation of an asymmetrical object

object in collaboration with the robot while a wrench was applied via multiple (left and right) time-invariant human contacts.

The following observations were drawn from the experimental results: Limiting the dissipated power at the human contact points was found to be a less conservative setting as the total dissipated power could be split among multiple human contact points and thus, a larger injected power could be admissible than when applying the threshold at the robot injection point. This can be observed in Fig. 4 between 12 s and 13 s, where the power at the robot side P_c exceeds the safety threshold of 1.5 W.

2) Cross-Contact Power Transfer in Multi-Contact Interaction: In addition to the aforementioned experimental

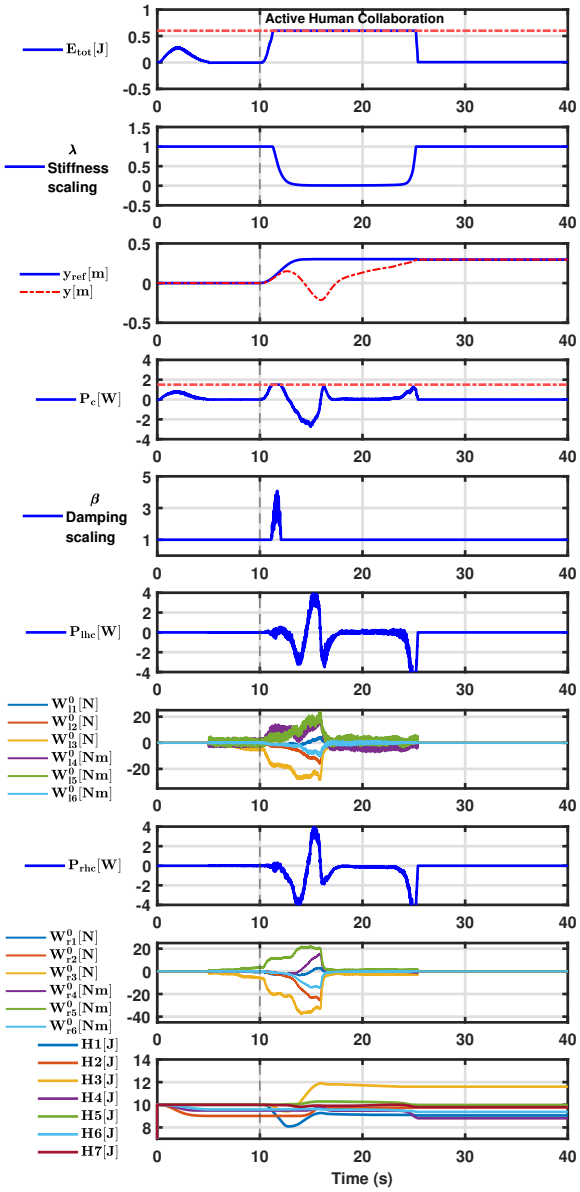

Fig. 5. Experimental results for limiting injected power at the robot contact point, with wrenches applied through multiple (left and right) time-invariant human contacts during the co-manipulation of an asymmetrical object

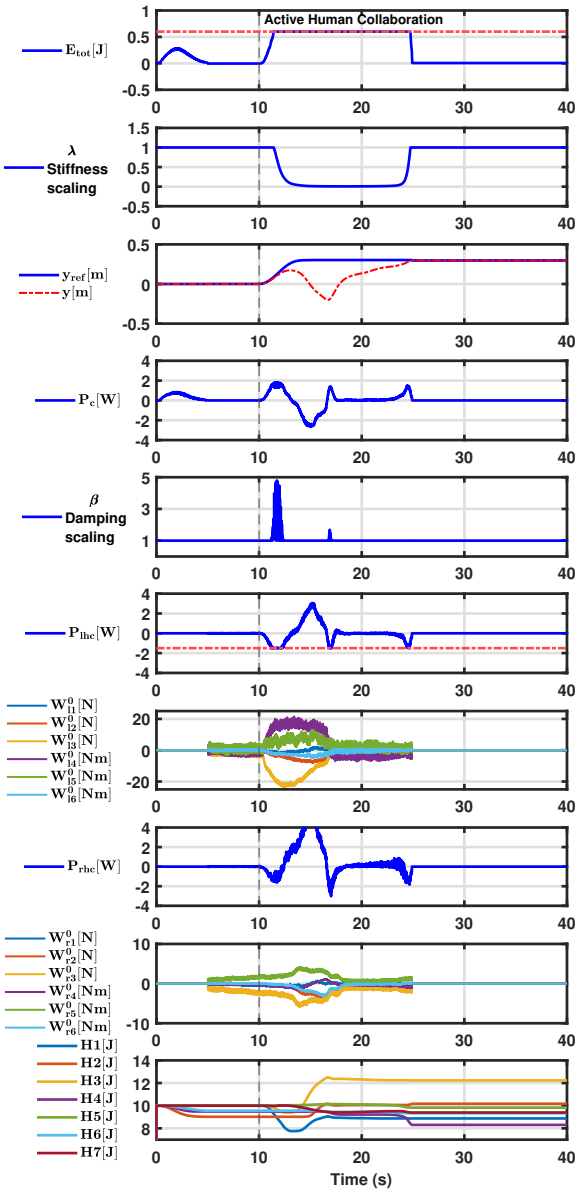

Fig. 6. Experimental results in case of safety limits applied to the left human contact only during co-manipulation of an asymmetrical object

analysis, the possibility of injecting power not only via the robot contact point, but also via one of the multiple human contact points as well as its effect on the to-be-dissipated power at the other human contact points was studied. This investigation is significant, as prior research typically focused on a single interaction point between humans and robot. However, with an increased number of contact points, as considered in the present work, power injected via one human contact point can also result in an excessive power to be dissipated at the other human contact point, highlighting a critical aspect of multi-contact interaction.

For this purpose, the human was asked to hold an asymmetrical object (see Fig. 2(c)) at multiple contact points and was instructed to interact actively with the robot when performing the co-manipulation task, while only the left human contact was subjected to safety limits, see Fig. 6.

It can be observed that at around 11 s, as soon as the power threshold for the human contacts is hit, the human operator takes control of the co-manipulation task, and power is injected by the human operator. At around 17 s, the power to be dissipated via the right human contact exceeds the safety thresholds due to the power injected at the left human contact. After 17 s, the robot tries to return to the desired trajectory using the available power in the system. However, at around 24 s the safe power to be dissipated via the right human contact is exceeded due to the attempt to decelerate the object.

These experiments highlight that the power to be dissipated at one human contact could also originate from power

injections via one of the other human contact points or changes in the potential and kinetic energy of the handled object. Therefore, limiting the dissipated power at multiple human contact points compared to limiting the injected power by the robot (as is the case in state-of-the-art implementations) is considered a safer strategy.

IV. CONCLUSIONS

An energy-shaping controller has been proposed to enhance safety in co-manipulation tasks with multiple, time-invariant human contact points. The controller effectively limits the energy stored in the system and manages energy flows (power) at these contact points by utilizing recharging and depleting energy tanks.

The proposed framework enhances safety by limiting dissipated power at multiple human–contact points, offering a less conservative safety strategy than conventional methods that restrict injected power at the robot side (see Section III-D.1 and Section III-D.2). In addition, controller versatility and adaptability has been validated through co-manipulation of symmetric and asymmetric objects of different masses emphasizing the applicability of the framework in human-robot collaboration and reinforcing its relevance for safety-critical applications beyond the specific validation presented.

The approach currently employs power thresholds derived from available safety norms, which, while suitable for developing and evaluating safety controllers [17], [18], [19], are based on experimental injury analyses [20], [21] related to impact situations. More research is needed to establish appropriate thresholds for continuous interaction scenarios involving multiple contact points. Besides, context-aware safety control could be explored by integrating real-time data to dynamically adjust energy limits based on the environment and task. Advanced models that incorporate human biomechanics could also improve energy dissipation management during interactions.

Moreover, the assumption of time-invariant contacts in this study is overly idealistic; future work should investigate time-varying contacts to enhance the realism of co-manipulation tasks.

The current work further assumes knowledge of contact locations and forces. While human contact locations can be measured using state-of-the-art vision techniques, force/torque sensors could be replaced by wearable sensors embedded in gloves, capable of measuring exerted human forces, as demonstrated in [22] and [23].

Finally, the potential impact of human muscle fatigue should also be considered, and the resulting controller should be evaluated in tasks that involve varying levels of exertion.

REFERENCES

[1] ISO 10218-2:2025 – robotics — safety requirements — part 2: Industrial robot applications and robot cells, 2025. Technical Specification ISO/TS 15066:2016 incorporated into ISO 10218-2:2025,.

[2] Martin Angerer, Selma Musić, and Sandra Hirche. Port-hamiltonian based control for human-robot team interaction. In *2017 IEEE International Conference on Robotics and Automation (ICRA)*, pages 2292–2299. IEEE, 2017.

[3] Milad Geravand, Erfan Shahriari, Alessandro De Luca, and Angelika Peer. Port-based modeling of human-robot collaboration towards safety-enhancing energy shaping control. In *2016 IEEE International Conference on Robotics and Automation (ICRA)*, pages 3075–3082. IEEE, 2016.

[4] Alessandro De Luca and Fabrizio Flacco. Integrated control for phri: Collision avoidance, detection, reaction and collaboration. In *2012 4th IEEE RAS & EMBS International Conference on Biomedical Robotics and Biomechatronics (BioRob)*, pages 288–295. IEEE, 2012.

[5] Sami Haddadin. *Towards safe robots: approaching Asimov's 1st law*, volume 90. Springer, 2013.

[6] Matteo Laffranchi, Nikos G Tsagarakis, and Darwin G Caldwell. Improving safety of human-robot interaction through energy regulation control and passive compliant design. *Human machine interaction-getting closer*, 2011.

[7] Johannes Lachner, Felix Allmendinger, Eddo Hobert, Neville Hogan, and Stefano Stramigioli. Energy budgets for coordinate invariant robot control in physical human–robot interaction. *The International Journal of Robotics Research*, 40(8-9):968–985, 2021.

[8] Tadele Shiferaw Tadele, Theo JA De Vries, and Stefano Stramigioli. Combining energy and power based safety metrics in controller design for domestic robots. In *2014 IEEE International Conference on Robotics and Automation (ICRA)*, pages 1209–1214. IEEE, 2014.

[9] Gennaro Raiola, Carlos Alberto Cardenas, Tadele Shiferaw Tadele, Theo De Vries, and Stefano Stramigioli. Development of a safety- and energy-aware impedance controller for collaborative robots. *IEEE Robotics and automation letters*, 3(2):1237–1244, 2018.

[10] Stefano Stramigioli. *Modeling and IPC control of interactive mechanical systems—A coordinate-free approach*. Springer, 2001.

[11] Antonio Franchi, Cristian Secchi, Hyoung Il Son, Heinrich H Bulthoff, and Paolo Robuffo Giordano. Bilateral teleoperation of groups of mobile robots with time-varying topology. *IEEE Transactions on Robotics*, 28(5):1019–1033, 2012.

[12] A Macchelli. *Port Hamiltonian systems. A unified approach for modeling and control finite and infinite dimensional physical systems*. PhD thesis, Ph. D. dissertation, University of Bologna–DEIS, 2003.

[13] Vincent Duindam, Alessandro Macchelli, Stefano Stramigioli, and Herman Bruyninckx. *Modeling and control of complex physical systems: the port-Hamiltonian approach*. Springer Science & Business Media, 2009.

[14] Philine Donner, Satoshi Endo, and Martin Buss. Physically plausible wrench decomposition for multieffector object manipulation. *IEEE Transactions on Robotics*, 34(4):1053–1067, 2018.

[15] Alexander Dietrich, Xuwei Wu, Kristin Bussmann, Christian Ott, Alin Albu-Schäffer, and Stefano Stramigioli. Passive hierarchical impedance control via energy tanks. *IEEE Robotics and automation letters*, 2(2):522–529, 2016.

[16] Tadele Shiferaw Tadele, Theo de Vries, and Stefano Stramigioli. Pid motion control tuning rules in a damping injection framework. In *2013 American Control Conference*, pages 4957–4962. IEEE, 2013.

[17] Antonio Bicchi and Giovanni Tonietti. Fast and" soft-arm" tactics [robot arm design]. *IEEE Robotics & Automation Magazine*, 11(2):22–33, 2004.

[18] Jochen Heinzmann and Alexander Zelinsky. Quantitative safety guarantees for physical human-robot interaction. *The International Journal of Robotics Research*, 22(7-8):479–504, 2003.

[19] Matteo Laffranchi, Nikolaos G Tsagarakis, and Darwin G Caldwell. Safe human robot interaction via energy regulation control. In *2009 IEEE/RSJ International Conference on Intelligent Robots and Systems*, pages 35–41. IEEE, 2009.

[20] Jack L Wood. Dynamic response of human cranial bone. *Journal of biomechanics*, 4(1):1–12, 1971.

[21] N Yoganandan, FA Pintar, DJ Maiman, JF Cusick, A Sances Jr, and PR Walsh. Human head-neck biomechanics under axial tension. *Medical engineering & physics*, 18(4):289–294, 1996.

[22] Xuguang Sun, Jianhai Sun, Tong Li, Shuaikang Zheng, Chunkai Wang, Wenshuo Tan, Jingong Zhang, Chang Liu, Tianjun Ma, Zhimei Qi, et al. Flexible tactile electronic skin sensor with 3d force detection based on porous cnts/pdms nanocomposites. *Nano-micro letters*, 11:1–14, 2019.

[23] Ayane Saito, Wakaba Kuno, Wataru Kawai, Natsuki Miyata, and Yuta Sugiura. Estimation of fingertip contact force by measuring skin deformation and posture with photo-reflective sensors. In *Proceedings of the 10th Augmented Human International Conference 2019*, pages 1–6, 2019.